Elucidating the impact of micro-scale heterogeneous bacterial distribution on biodegradation

Schmidt, Susanne; Kreft, Jan-Ulrich; Mackay, Rae; Picioreanu, Cristian; Thullner, Martin

DOI:
10.1016/j.advwatres.2018.01.013

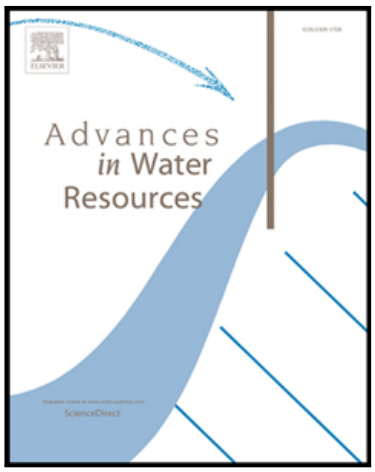

Elucidating the impact of micro-scale heterogeneous bacterial distribution on biodegradation

Susanne I. Schmidt , Jan-Ulrich Kreft , Rae Mackay , Cristian Picioreanu , Martin Thullner

PII: S0309-1708(17)30730-3
DOI: 10.1016/j.advwatres.2018.01.013
Reference: ADWR 3069

To appear in: *Advances in Water Resources*

Received date: 20 July 2017
Revised date: 11 January 2018
Accepted date: 15 January 2018

Please cite this article as: Susanne I. Schmidt , Jan-Ulrich Kreft , Rae Mackay , Cristian Picioreanu , Martin Thullner , Elucidating the impact of micro-scale heterogeneous bacterial distribution on biodegradation, *Advances in Water Resources* (2018), doi: 10.1016/j.advwatres.2018.01.013

Highlights

- The heterogeneous micro-scale microbial growth in pores reduces bioavailability
- This growth form can reduce degradation rates by up to an order of magnitude.
- Effective mass transfer rates for such limited biodegradation are derived.
- A conceptual approach how these results may be scaled up is provided for two substances: acetate and toluene.

Elucidating the impact of micro-scale heterogeneous bacterial distribution on biodegradation

Susanne I. Schmidt[a,1*], Jan-Ulrich Kreft[b], Rae Mackay[c], Cristian Picioreanu[d], Martin Thullner[e]

[a] Centre for Systems Biology, University of Birmingham, UK; schmidt-s@uni-landau.de

[b] Centre for Computational Biology & Institute of Microbiology and Infection & School of Biosciences, University of Birmingham, UK; J.Kreft@bham.ac.uk

[c] Faculty of Science and Technology, Federation University, Gippsland, Gippsland Mail Centre VIC 3841, Australia; rae.mackay@federation.edu.au

[d] Department of Biotechnology, Faculty of Applied Sciences, Delft University of Technology, The Netherlands; C.Picioreanu@tudelft.nl

[e] Department of Environmental Microbiology, UFZ – Helmholtz Centre for Environmental Research, Leipzig, Germany; martin.thullner@ufz.de

* Corresponding author: Susanne I. Schmidt schmidt-s@uni-landau.de

[1] Present address: Institute for Environmental Sciences, University of Koblenz-Landau, Germany

Abstract

Groundwater microorganisms hardly ever cover the solid matrix uniformly–instead they form micro-scale colonies. To which extent such colony formation limits the bioavailability and biodegradation of a substrate is poorly understood. We used a high-resolution numerical model of a single pore channel inhabited by bacterial colonies to simulate the transport and biodegradation of organic substrates. These high-resolution 2D simulation results were compared to 1D simulations that were based on effective rate laws for bioavailability-limited biodegradation. We i) quantified the observed bioavailability limitations and ii) evaluated the applicability of previously established effective rate concepts if microorganisms are heterogeneously distributed. Effective bioavailability reductions of up to more than one order of magnitude were observed, showing that the micro-scale aggregation of bacterial cells into colonies can severely restrict the bioavailability of a substrate and reduce *in situ* degradation rates. Effective rate laws proved applicable for upscaling when using the introduced effective colony sizes.

Key words

pore-scale microbial degradation; bioavailability; effective rate laws; upscaling

1. Introduction

Microbial degradation of organic compounds in groundwater is one of the most important processes controlling the fate of chemicals in the subsurface. In particular, natural attenuation and contaminant remediation commonly rely on this microbial ecosystem service, which emphasizes its relevance for environmental quality and water resources management [1], [2]. It is thus important to know where exactly, and under which circumstances, microbial degradation occurs, and how it can be promoted most effectively. For this, knowledge of the factors limiting *in situ* biodegradation rates is crucial.

One important factor that controls the dynamics of *in situ* biodegradation in porous aquifers is the bioavailability of the substrate to the microorganisms [3], [4], which can lead to significant differences between *in situ* degradation rates observed for porous media and rates observed for ideal laboratory conditions [5]. Pore-scale mass transfer has been identified as an important process limiting the bioavailability of a substrate in a porous medium [6]–[8]. The majority of groundwater microorganisms are not found freely floating in the pore water but attached to the pore walls, i.e. the surface of the solid matrix [9]–[13]. Since groundwater flow in porous media is laminar, micro-scale advective transport to the attached microorganisms is restricted. Thus, microorganisms rely on diffusive mass transfer to the cells. Furthermore, it is now well known that microbes are not evenly spread along the pore walls, but their distribution is patchy [14] and, usually, microcolonies are formed [15]. In groundwater, microcolonies typically contain 100 cells or fewer [9].

The relevance of micro-scale mass transfer of substrate to the microorganisms imposes severe challenges for a quantitative assessment of biodegradation rates [6], [16]–[18]. In parallel to fine-scale sampling, models – once verified and validated – may be used as prediction and decision tools in order to steer groundwater resource management in the most effective and efficient way. However, the biodegradation rates applied in these models must consider all processes potentially limiting *in situ* degradation. While the micro-scale heterogeneity of the distribution of microorganisms has been acknowledged already in early modelling studies [19], [20], micro-scale mass transfer limitations are either not considered or based on effective rate expressions, the parameters of which are poorly constrained [21]. More recently, approaches combining high-resolution pore-scale descriptions with upscaling theory have led to an improved understanding of the link between the geometry of the pore space, effective rate expressions for mass transfer limited biodegradation and quantitative estimates of the associated effective rate parameters [16], [17], [22]–[24]. In particular, the Best equation [25], a combination of a linear exchange term linking bulk and bioavailable concentrations with Michaelis-Menten kinetics for the bacterial metabolism, has been verified as an appropriate effective rate law with mass transfer coefficients derived from the pore sizes and the diffusivity of the substrate [17]. However, these approaches and their conclusions regarding the magnitude of the mass transfer limitations are based on the assumption that the microorganisms are covering the pore walls evenly as a film-like biofilm of constant thickness. While this conceptual simplification facilitates the derivation of closed-form effective rate expressions and provides a link to models applied to abiotic, surface-catalysed reactions in porous media [26]–[28], it might fail to describe effective rates in case of heterogeneous colony-like distributions of microbial cells. Other well established

approaches to effective boundary expressions include homogenization techniques [29] or (heterogeneous) multiscale modeling [30], as well as rough reactive walls concept [31], reviewed in [32], focus on the heterogeneity of the surface structure rather than on the heterogeneity of the reactivity. Such formulation allows for a mathematically closed form and renders numerical calculations unnecessary. This is adequate where the knowledge of average properties is sufficient and details on the flow at the roughness scale are not required, and where a steady state for the geometry is reached and does not evolve anymore. No effective rate approaches currently exist that consider a heterogeneous micro-scale distribution of the microorganisms forming colonies or micro-aggregates instead of evenly covering the pore walls. It is therefore not known to which extent the tendency of the microorganisms to form such colonies affects the bioavailability and thus biodegradation of a substrate.

The main aim of this paper is therefore to examine to what extent colony-wise microbial distribution decreases bioavailability and degradation in pores. For this purpose, we couple the fluid dynamics and substrate transport with an individual-based model (IbM; [33]) of bacterial colonies to simulate the reactive transport of organic substrates within a pore channel. These computations are combined with upscaled simulations using effective rate laws, which allows for i) quantification of the observed bioavailability limitations and ii) evaluation of the applicability of previously established effective rate concepts in the more realistic case of heterogeneously distributed microorganisms.

2. Methods

We performed two-dimensional (2D) finite element (FE) simulations and one dimensional (1D) simulations of fluid flow and solute transport with reaction in a pore channel in order to show the effect of microbial cell distribution on the degradation of a dissolved substrate. The modelled domain had a length $L_x = 10^{-3}$ m (Table 1) and represented a 2D cross-section of a pore channel in flow direction (schematic overview in Figure 1). Only one half of the cross-section was simulated (height $L_y = 10^{-4}$ m; Table 1), assuming symmetry in the other half. Gradients were considered to be absent along the z direction.

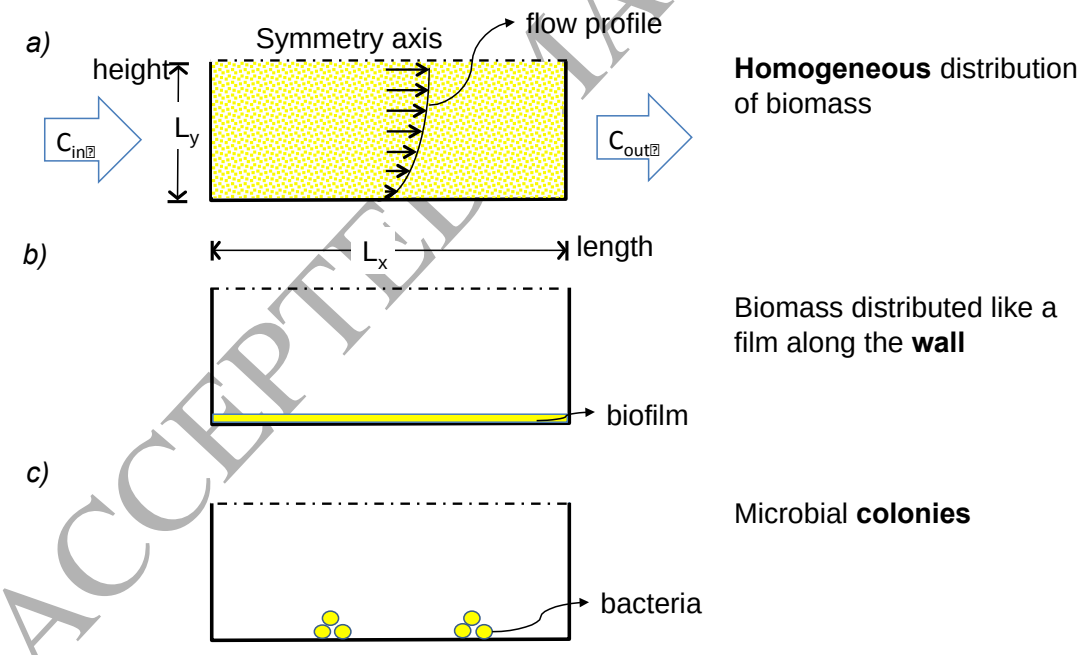

Figure 1: Schematic setup of the three types of simulation scenarios. a) Homogeneous distribution of biomass suspended in the aqueous phase, posing no resistance to flow; b) Biomass distributed along the pore wall like a thin continuous biofilm of uniform thickness, quasi-impermeable to flow; c) Discrete colonies formed by spherical cells aggregated in one to eight colonies on the wall of the pore channel. Left boundary: laminar flow profile with a set average velocity and fixed concentration; Lower boundary: impermeable wall (zero flow (no slip), zero solute flux normal to the surface); Upper boundary: symmetry axis; Right boundary: set pressure and zero diffusive flux perpendicular to the boundary.

Parameter	Description	Value	Unit	Source
Geometry				
L_x	System dimension along the length	10^{-3}	m	
L_y	System dimension along the height	10^{-4}	m	
Dissolved components				
$c_{0,ac}$	Inlet concentration acetate	0.162	$g_{acetate} \cdot m^{-3}$	[34]
$c_{0,tol}$	Inlet concentration toluene	1.8	$g_{toluene} \cdot m^{-3}$	SI 2
$D_{m,ac}$	Diffusion coefficient acetate	$8.35 \cdot 10^{-10}$	$m^2 \cdot s^{-1}$	SI 1
$D_{m,tol}$	Diffusion coefficient toluene	$6.30 \cdot 10^{-10}$	$m^2 \cdot s^{-1}$	SI 1
u_{in}	Average inlet velocity	$1.25 \cdot 10^{-6}$ to $40 \cdot 10^{-6}$	$m \cdot s^{-1}$	chosen to represent groundwater velocity
$\rho_{water,\ 10°C}$	Density of water at 10°C	999.7027	$g \cdot m^{-3}$	[35]
$\mu_{water,\ 10°C}$	Viscosity of water at 10°C	$1.31 \cdot 10^{-3}$	$Pa \cdot s$	[36]
Biomass components				
ρ_X	Dry biomass density of bacterial cells	200,000	$g \cdot m^{-3}$	Assuming biomass density to be equal to water and biomass to be 80% water
V_X	Constant volume of bacterial cells	10^{-18}	m^{-3}	Groundwater cell volume rounded up from Griebler et al. [12]
Microbial rate parameters, calculated for 10°C ambient temperature				
Y_{ac}	Yield for bacterial oxidation of acetate	0.353	$g_{drymass} \cdot g_{toluene}^{-1}$	[37]
Y_{tol}	Yield for bacterial oxidation of toluene	1.2	$g_{drymass} \cdot g_{acetate}^{-1}$	[38]
$k_{max,ac}$	Specific reaction rate for bacterial oxidation of acetate	$13 \cdot 10^{-5}$	$g_{acetate} \cdot g_{drymass}^{-1} \cdot s^{-1}$	SI 1
$k_{max,tol}$	Specific reaction rate for bacterial oxidation of toluene	$6.3 \cdot 10^{-5}$	$g_{toluene} \cdot g_{drymass}^{-1} \cdot s^{-1}$	SI 1, SI 2
$K_{s,ac}$	Michaelis-Menten half-saturation coefficient for acetate oxidation	0.101	$g_{acetate} \cdot m^{-3}$	SI 1
$K_{s,tol}$	Michaelis-Menten half-saturation coefficient for toluene oxidation	0.0544	$g_{toluene} \cdot m^{-3}$	SI 1, SI 2

Table 1: Parameters used in the models, considering the typical groundwater temperature of 10°C. Sources are listed where values were directly taken from the literature, otherwise the derivation of the parameters is explained in the SI. Some of the parameters only apply to the COMSOL simulations.

2.1 2D simulations – general setup

This model was implemented in a combination of MATLAB (www.mathworks.com) code with Java (www.java.com) and COMSOL Multiphysics 3.5 (Comsol, Stockholm, Sweden, www.comsol.com). A homogeneously spatially discretized, rectangular 2D grid with square grid cells of side length of $2 \cdot 10^{-6}$ m was defined in MATLAB. In this proof-of-principle study, the biomass distribution was defined only once in MATLAB and cells were not growing (pseudo-equilibrium simulation). Different biomass distribution patterns were considered (see Figure 1): i) homogeneous distribution of biomass suspended throughout the aqueous phase; all of the grid cells were assigned solute viscosity, but at the same time, the total biomass was evenly allocated into all grid cells, not only to those along the wall. ii) For scenarios considering a continuous biofilm of uniform thickness along the pore walls, the total biomass was divided equally into all wall-bound grid cells so that each wall-bound grid cell received biomass. Therefore, in this wall type scenario, all wall-bound grid cells were attributed the same viscosity as those grid cells containing colony cells. This led to a flow profile with a decreased flow velocity close to the wall. iii) In the case of discrete colonies of cells on the wall, microcolonies were generated with an individual-based algorithm [39] from single cells placed at pre-determined points along the pore walls that were far enough from the pore inlet and outlet so as not to be influenced by edge effects from pore ends. The algorithm divided cells stepwise, until the desired total cell number of the colony was reached (details on the spatial allocation of the new cells are given in Lardon et al. [33] and Kreft et al. [40]; the positions of the cells were adjusted to avoid overlap, using the shoving algorithm described by Picioreanu et al. [41]). This algorithm was implemented in Java and

called from MATLAB. After this, the positions and sizes of the cells were constant and no further growth of biomass was considered during the simulations.

After the colony-generating or equivalent steps, two matrices were set up: one matrix held the biomass concentrations for each grid cell, which was used for calculating reaction rates, and a second matrix held the viscosities for each grid cell. Biomass-free grid cells were defined as belonging to the liquid compartment and their viscosity was set to the value for water at 10°C of $1.31 \cdot 10^{-3}$ Pa·s [36]. We set the fluid in these cells to be incompressible and the flow unidirectional. Biofilms and biocolonies consist of cells and extracellular polymeric substance (EPS) which itself has a gel-like consistency [42]. Wet densities of both biomass and EPS are roughly the same [42]. We treated the biofilm and colonies as an incompressible viscous Newtonian fluid [14], [43]–[46] and set the viscosity of biomass-containing grid cells to $1 \cdot 10^{4}$ Pa·s (~10^{7} times the value for water), in order to make sure that only diffusion takes place inside the biofilm, but no flow.

Based on the channel geometry thus formed, the stationary laminar flow field and the steady-state concentration distribution of substrate were computed by solving an advection-diffusion-reaction equation using COMSOL Multiphysics 3.5a, called with the MATLAB code. The model geometry, biomass and viscosity matrices as well as parameters (Table 1; kinetics derived in SI 1 and 2) were imported into COMSOL. The Matlab matrices were represented in COMSOL by two-dimensional interpolation of the rectangular Matlab grid. The substrate degradation in the regions occupied by biomass was described by Michaelis-Menten type kinetics considering only one rate-limiting substrate (Table 1). The spatial substrate distribution and the flow field were

calculated by solving the laminar flow simplified Navier-Stokes equation, as well as the diffusion-reaction mass balance on a finite element mesh generated in COMSOL with the default settings. For this, a no-slip condition (zero velocity) was applied at the pore wall, while flow symmetry was assumed at the upper boundary of the simulated domain (Figure 1). A constant pressure was considered at the outlet boundary, while a fully developed (i.e. parabolic) laminar flow velocity profile was set at the inlet boundary, by setting a length of the inlet channel outside the model domain sufficiently long for a laminar flow profile to have developed (i.e. parabolic flow profile) at the inlet (Figure 1). The inflow received the set concentration at the velocity specified from the coupled Navier-Stokes equation. The lower (solid wall) and upper (symmetry) axes were set to zero flux normal to the surface, and the outflow was set to convection-only substrate transport. The mass balances were solved, with ε in the Navier-Stokes equation, *i.e.* the rate-of-strain tensor, having been derived from the viscosity grid. Results averaged for each finite element, including substrate concentrations and internal stresses, were returned to Matlab following an operator-splitting procedure [47] – in the present study these values were only applied to derive the graphical representations, but in future applications of this framework, these returned values will be used for simulating the temporal development of the bacterial colonies. The steps from creating the matrices for biomass and viscosity based on the microbial growth up to solving the laminar flow simplified Navier-Stokes equation, as well as the diffusion-reaction mass balance and growing bacteria according to the new velocity and substrate field, can be iterated over for resolution in time. Similar procedures were used previously [48]–[51]. The graphical representations were prepared using R [52], in particular packages ‘lattice’ (v. 0.20-34 [53]) and ‘ggplot2’ (v. 2.2.2 [54]).

2.2 1D simulations

Processes in the pore channel were also simulated by combining a one-dimensional (1D) description of flow and transport along the length of the pore with an effective degradation rate that considered the spatial arrangement of the biomass in the pore. The length of the pore channel, the 1D spatial discretization along the pore length and the in- and outflow boundary conditions were the same as for the 2D simulations. Flow velocity was constant along the pore length and corresponded to the average flow velocity in the 2D simulations.

For a homogeneous biomass distribution in the aqueous phase, substrate degradation was described by Michaelis-Menten kinetics analogous to the 2D simulations. For scenarios with biomass covering the pore wall as a thin, constant thickness biofilm, the effective rate was described by Heße et al. [16], [17] who showed that the combination of a linear mass transfer term with Michaelis-Menten degradation kinetics can adequately describe the diffusive mass transfer towards the pore wall, where microbial degradation takes place. The resulting combined rate expression is known as the Best equation [25]:

$$r_{eff,Best} = \frac{K_s \cdot k_{tr}}{2}\left(1 + \frac{c}{K_s} + \frac{k^*_{max}}{K_s \cdot k_{tr}}\right) \cdot \left(1 - \sqrt{1 - \frac{4\frac{c}{K_s}\frac{k^*_{max}}{K_s \cdot k_{tr}}}{\left(1+\frac{c}{K_s}+\frac{k^*_{max}}{K_s \cdot k_{tr}}\right)^2}}\right) \quad (1)$$

where c is the concentration of substrate and K_s is the Michaelis-Menten half-saturation coefficient for the substrate. Values for the maximum reaction rate $k^*_{max} = k_{max} \cdot c_{bac}$ were derived from the maximum specific reaction rates k_{max} and the average bacterial biomass concentration in the simulated pore channel ($c_{bac} = m_X \cdot N_{bac}/V_{pore}$ where N_{bac} is the number of bacterial cells in the domain and the pore volume given as $V_{pore} = L_x \cdot L_y \cdot d_z$, where d_z is a thin layer of $2 \cdot 10^{-6}$ m; m_x is the bacterial mass, derived from the volume of the bacterial cells V_x and dry biomass density ρ_x). The mass transfer coefficient, $k_{tr} = \frac{\pi^2}{4} \cdot \frac{D_m}{L_y^2}$ [17] depends on the molecular diffusion coefficient D_m and the height L_y of the simulated pore channel.

We adapted this approach to describe the presence of microbial colonies (i.e. discontinuous distributions of biomass along the pore wall). An effective size (length) was attributed to the colonies (same value for each colony) and the degradation activity was restricted to individual, discontinuous sections of the pore length, the position of each section given by the location and effective size of the colonies. Within these sections, the biomass of the corresponding colony was considered to be continuously distributed along the pore wall. Compared to the continuous biofilm case described by the Best equation, the value of k^*_{max} is elevated by a factor $F = \frac{L_x}{N_c \cdot d_c}$ due to the increased biomass concentration in the colony sections, where L_x is the length of the pore, N_c the number of colonies in the pore and d_c the effective colony size. Outside these sections, k^*_{max} is set to zero. Furthermore, an alternative description was considered assuming degradation to take place continuously along the entire pore length. To account for the aggregation of cells in the colonies k^*_{max} was again

increased by the factor *F*, but subsequently the resulting rate was divided by *F* since the wall was covered by the biomass only in a fraction 1/F of pore length.

The 1D model was implemented in the Biogeochemical Reaction Network Simulator (BRNS; [55], [56]) Transient simulations were performed until a steady state was reached. All parameters describing the reactive transport had the same value as in the 2D simulations or were directly derived from them. The only exception was the effective colony size d_c, which was fitted for each individual scenario to achieve a maximal match between the 1D and 2D simulation results. For this comparison, 2D concentration distributions *c(x,y)* were averaged across the height of the simulated pore channel using flux-weighted averages:

$c_{average,flux}(x) = \frac{\int_y c(x,y) \cdot u(x,y) dy}{\int_y u(x,y) dy}$ with $c_{average,flux}(x)$ as average concentration and *u(x,y)* as pore water velocity.

Results of the 1D simulations were used to determine the effective bioavailability B_{eff} of the substrate for the different distributions of the bacterial cells [57]:

$$B_{eff} = \frac{r_{eff,Best}}{r_{MM}} \quad (2)$$

with $r_{MM} = k^*_{max} \cdot \frac{c}{c+K_s}$ given by Michaelis-Menten kinetics considering a homogeneous distribution of the cells in the aqueous phase without bioavailability restrictions. The effective rate is given according to Eq. 1 for a biofilm-like distribution along the pore wall or by using Eq. 1 with an elevated value of k^*_{max} based on the fitted effective colony sizes.

2.3. Simulated scenarios

Simulations were performed for different combinations of transport and degradation conditions. Average flow velocities in the pore inlet covered a range of $1.25 \cdot 10^{-6}$ m s^{-1} (0.108 m day^{-1}) to $20 \cdot 10^{-6}$ m s^{-1} (1.73 m day^{-1}). Groundwater bacterial cells usually have a – rounded up – volume V_X of 10^{-18} m^3 [58]. We set the dry biomass density ρ_X = 200,000 $g \cdot m^{-3}$, assuming wet biomass density equal to the density of water, 1,000,000 $g \cdot m^{-3}$, and the water content of biomass to be 80% (Table 1). The microbial cell numbers were varied from 50 to 800 cells/domain, which would be equivalent to a range from $7.5 \cdot 10^{13}$ to $1.2 \cdot 10^{15}$ cells m^{-3} aquifer material (assuming a porosity of 30%; see SI 2). These single pore values are largely in agreement with measured values (averaged for larger sampling volumes). For pristine aquifers, densities of $1.8 \cdot 10^{12}$ to $2.3 \cdot 10^{14}$ cells m^{-3} were reported [59], [60]. In contaminated aquifers, densities of $6 \cdot 10^{12}$ and $1.5 \cdot 10^{14}$ cells m^{-3} were reported [61], [62].

Simulations were performed for two different organic substrates with different degradability: acetate and toluene. Acetate was chosen as an easily degradable, ubiquitous substrate involved in a large variety of reaction pathways, occurring naturally both as a product from catabolic [63] and anabolic reactions [64], and generally as a reaction partner [65], [66]. Toluene was chosen as a common, environmentally significant representative of hydrocarbon contaminants [67], widely studied both at spill sites [68], [69] and in the laboratory [70]–[73]. A large excess of the electron acceptor was assumed, thus not affecting the degradation rates. The degradation rates for each compound (Table 1) at 10°C were adapted from the literature (see SI 1 and SI 2 for details).

For a base case scenario, an average flow velocity of u_{in} = $5 \cdot 10^{-6}$ m s^{-1}, 200 cells/domain, and acetate as substrate with an inlet concentration of 0.16 g m^{-3} were chosen. In all other scenarios one of these parameters was varied while keeping the others fixed. For the longitudinal transport along the pore channel the combination of parameters corresponds to Péclet numbers ($Pe = \frac{L_x u_{in}}{D_m}$) of 1.5 to 24 for acetate and 8 for toluene. The resulting Damköhler numbers ($Da = \frac{{k^*}_{max}/K_S}{u_{in}/L_x}$) are between 13 and 210 for acetate and 47 for toluene, respectively.

3. Results

The 2D simulation results for the base case scenario (acetate as substrate) show that changing the distribution of biomass affected the concentration distribution within the pore channel (Figure 2). The more aggregated the biomass was, the more pronounced the local micro-scale gradients were toward the location of the biomass aggregates. The latter led to a strong deviation between the substrate concentration at the location of the biomass and the concentration averaged across the height of the pore channel. As a consequence, the concentrations toward the outlet increased with increasing aggregation, indicating a decreasing overall degradation rate due to the aggregation. The same qualitative behaviour was observed with toluene as a substrate, different total cell number or average flow velocity (SI 3).

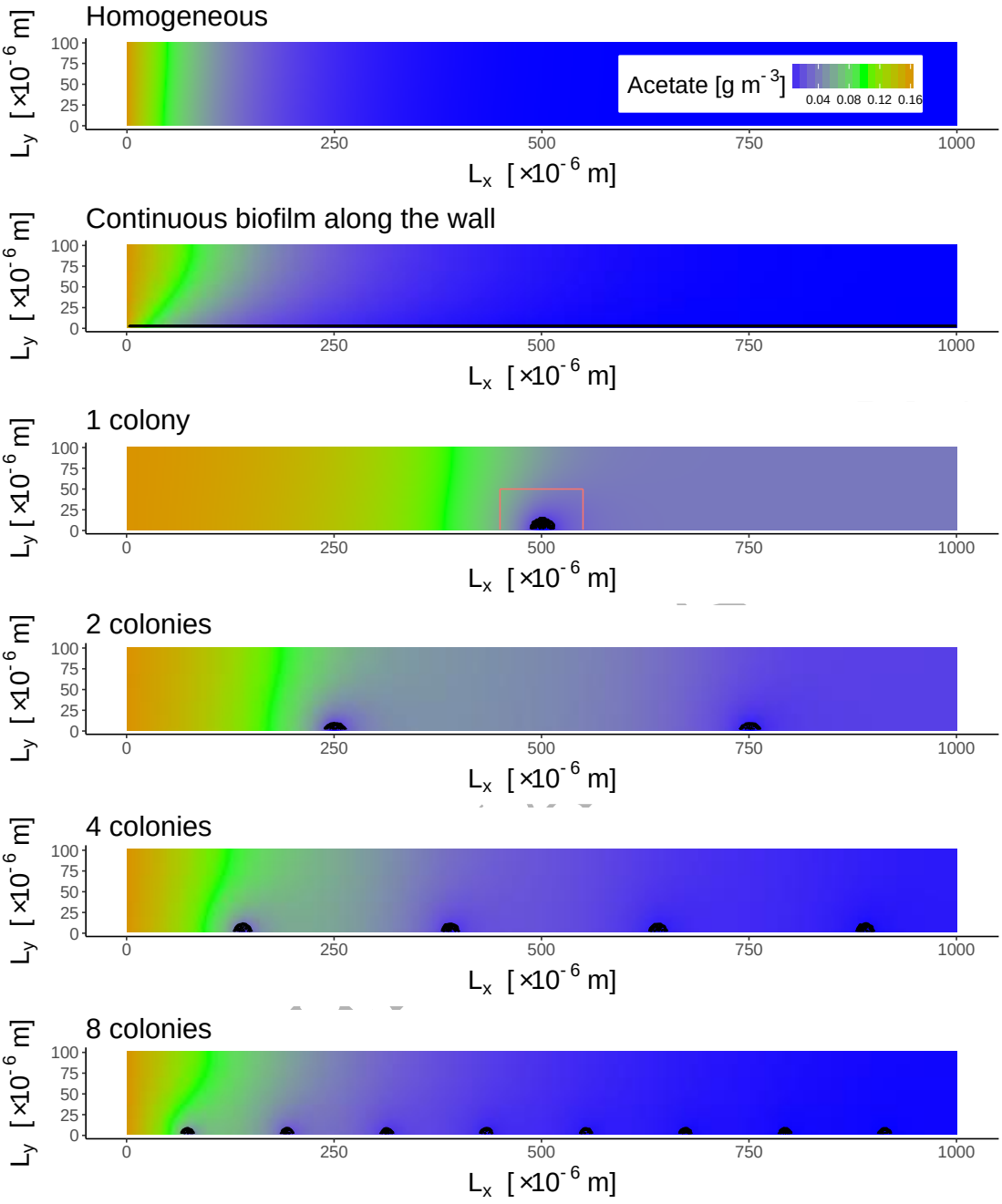

Figure 2: Computed steady state concentration distributions within a pore channel, for different biomass distribution models. These 2D simulation results are for the base case scenario (flow velocity $5{\cdot}10^{-6}$ $m{\cdot}s^{-1}$, 200 cells/domain, acetate as substrate). Homogeneous = uniform concentration of biomass suspended in liquid; Wall = continuous biofilm with uniform thickness along the pore wall; Colonies = the same total biomass aggregated into 1, 2, 4, or 8 equidistant colonies, respectively. The section within the red box is enlarged in SI Figure 4.

Degradation activity of the colonies was not restricted to the interface between biomass and pore water but substrate penetrated into the colonies (exemplary results shown in Figure 3 and Figure SI 4). The latter had an approximately semi-circular

cross section with radii varying between r_c = 2 µm for the smallest and r_c = 28 µm for the largest considered colonies. Using these colony sizes, values for the Thiele modulus ($\Phi^2 = \frac{k^*_{max}/K_s}{D_m/r_c^2}$; i.e. second order Damköhler number for comparison of time scales for degradation relative to diffusive transport) in the colonies ranged between 0.6 and 80, which broadly falls within the transition between diffusion and reaction limited regimes [16], [22].

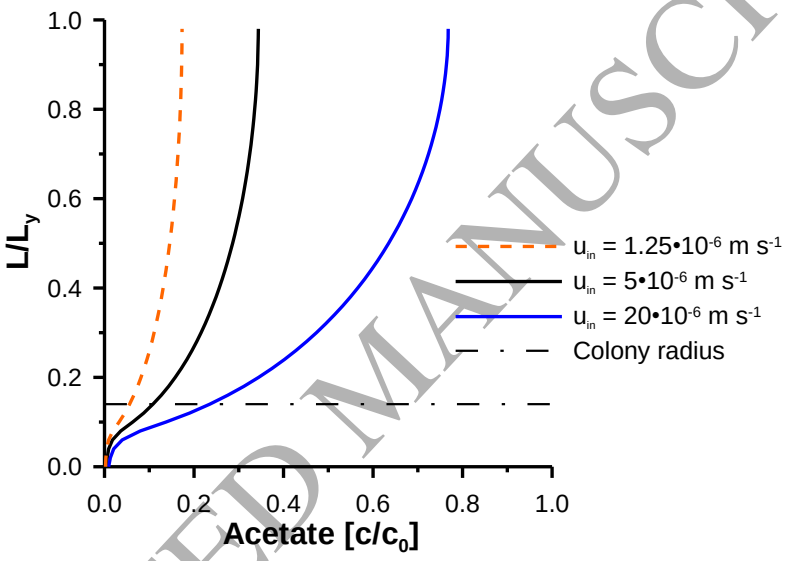

Figure 3: Acetate concentration profiles along L_y at the L_x position of the centre of one colony (line for colony radius marks interface between biomass and pore water) of 200 cells for the base case with different velocities.

Results of the 2D simulations were converted into 1D profiles showing the flux-weighted average concentration along the length of the pore channel (Figure 4). Note that an unweighted volumetric concentration averaging procedure led to nearly identical 1D profiles (SI 5). The profiles shown in Figure 4 were used as references for the 1D simulations. Results from the two simulation approaches for the homogeneous biomass distribution were in exact agreement. Also for the continuous

biofilm covering the pore walls, the 1D simulation results using the Best equation, with the mass transfer coefficient as predicted [17], were nearly identical to those from the 2D simulations. In scenarios with microbial colonies, the effective colony sizes were adjusted to fit the outlet concentrations of the 2D simulations (refer to section "1D simulation" in the method section). In the case of discontinuous reactive sections developed here, the obtained 1D profiles were also similar to the 2D simulation results. Results of the base case scenario are shown in Figure 4. Results of the other scenarios exhibited a similar agreement between 1D and 2D simulations (SI 6).

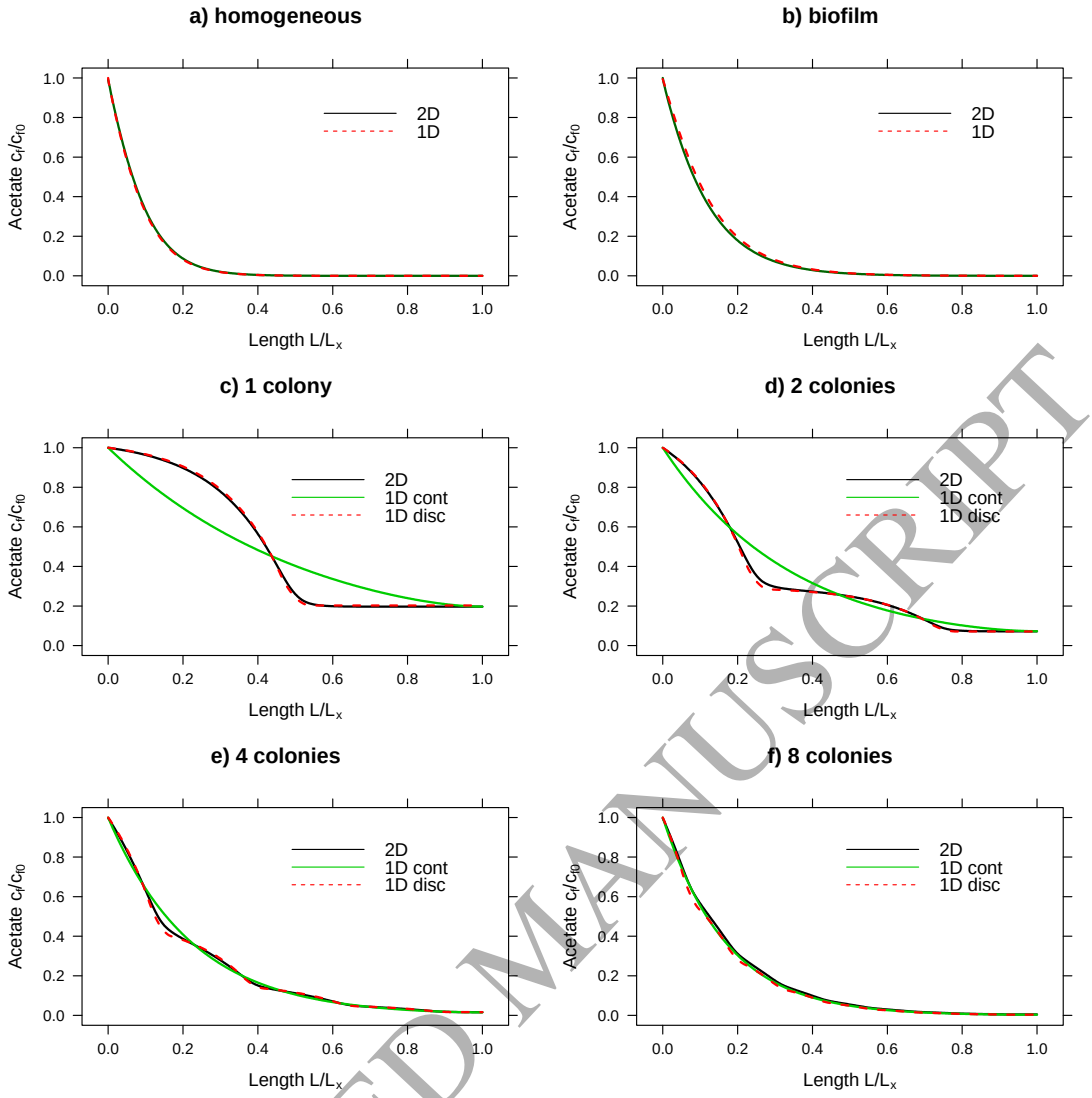

Figure 4: Flux-weighted concentration profiles comparing the 2D simulations (averaged over the cross-section of the pore channel) with 1D simulations using effective rate descriptions. Results are shown for the base case scenario (flow velocity $5{\cdot}10^{-6}$ m·s^{-1}; 200 cells/domain, acetate as substrate) and different biomass distributions: a) homogeneous in the liquid phase, b) continuous biofilm of uniform thickness along the pore wall, c)-f) biomass aggregated in 1, 2, 4, or 8 equidistant colonies, respectively; 'disc' refers to the effective rate expression for discontinuous reactive sections along the pore while 'cont' refers to the effective rate expression for one continuous reactive section along the entire pore.

The values of the effective colony sizes depended on the effective rate expressions used (several separate reactive sections vs. one continuous reactive section along the entire pore length): for the discontinuous case, values ranged between $36{\cdot}10^{-6}$ m and $140{\cdot}10^{-6}$ m, while for the continuous case the range was $36{\cdot}10^{-6}$ m to $92{\cdot}10^{-6}$ m (Figure 5). For the discontinuous case, the effective colony sizes clearly increased

with the number of cells/colony while other factors (flow velocity, total number of cells in the pore channel, substrate concentration and reactivity) caused only minor variations. Similar, although less pronounced, behaviour was observed for the continuous biomass distribution. Depending on the obtained effective colony sizes, the effective reactivity due to the biomass aggregation increased by up to one order of magnitude. The resulting effective bioavailability (i.e. the ratio of the effective, bioavailability-limited rate and the rate in absence of any restrictions [57] shows that the biomass aggregation led to substantial reductions of the effective bioavailability (Figure 6). Such substantial reductions of the effective bioavailability due to aggregation of cells into discrete colonies were also observed in cases where the continuous distribution of these cells along the pore wall would have led to minor effects only (Figure 6).

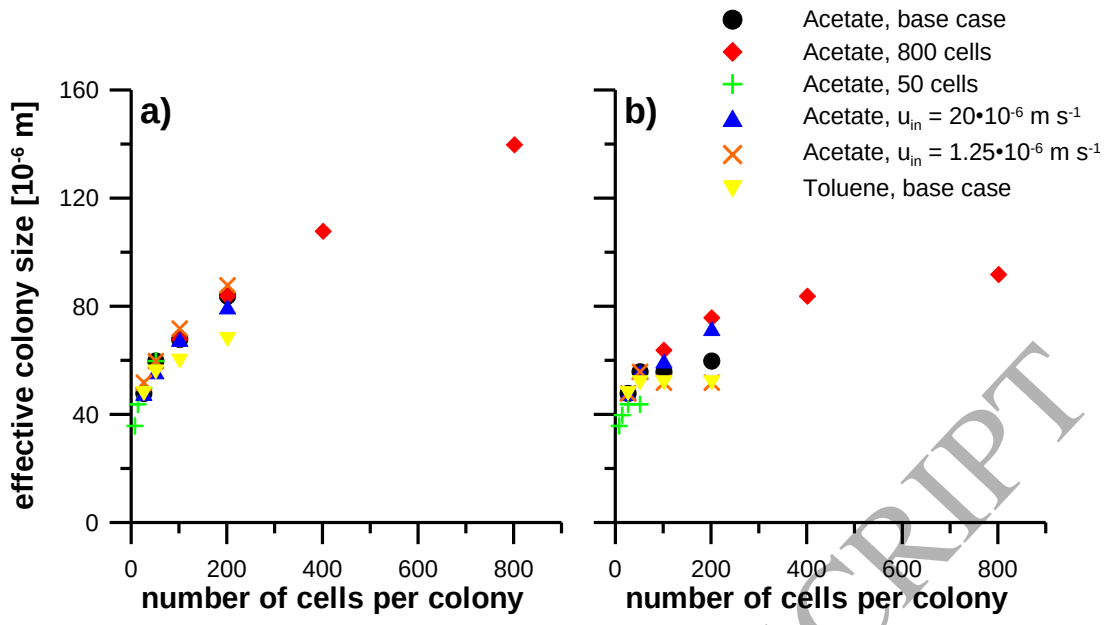

Figure 5: Effective colony size as a function of number of cells/colony both for a) discontinuous and b) continuous distribution of reactive sections along the pore wall in the 1D simulations. For the base case scenario, a flow velocity of $5 \cdot 10^{-6}$ m s^{-1}, 200 cells/domain and acetate or toluene as substrate were chosen.

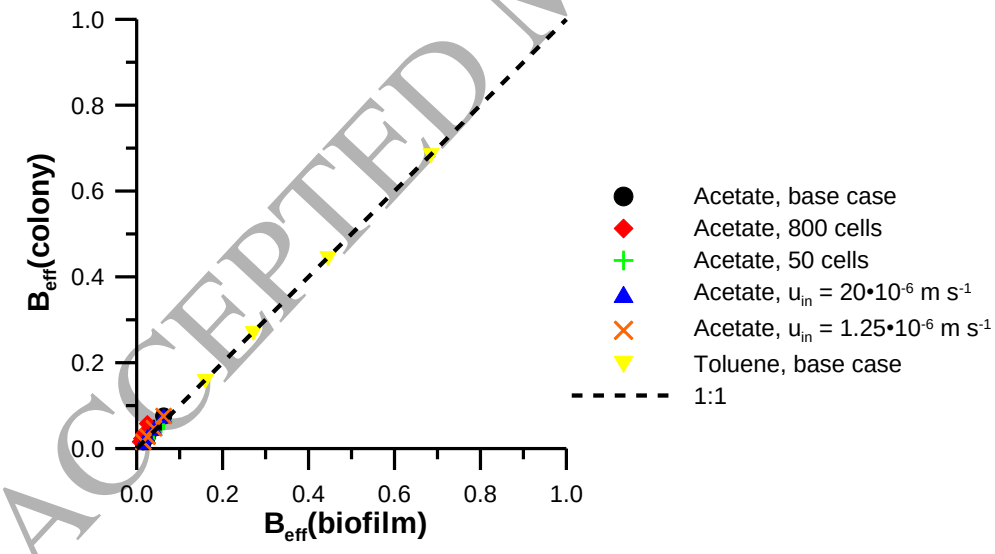

Figure 6: Effective bioavailability in scenarios with biomass aggregated into colonies compared with the same scenarios with a homogeneous biofilm-like coverage of the pore walls. For each vertical group of symbols, the lowest B_{eff}(colony) values are for 1 colony followed by values for 2, 4 and 8 colonies. Note that B_{eff} values of 1 indicate no bioavailability restrictions, while decreasing values indicate an increasing restriction. The 1:1 line indicates cases where aggregation into colonies does not lead to higher bioavailability restrictions than for a continuous biofilm. These results were calculated according to Eq. 2 with substrate concentrations equal to 50% of the inlet concentrations. For the base case scenario, a flow velocity of $5 \cdot 10^{-6}$ m s^{-1}, 200 cells/domain and acetate or toluene as substrate were chosen.

4. Discussion

The results of this study indicate that heterogeneity of biomass distribution can markedly affect pore-scale degradation. While this is in general agreement with previous studies [24], [43], [74]–[79], we were able to quantify the effects of biomass aggregations into colonies, which are acting as individual micro-scale hot spots of biodegradation. Such micro-scale hot spots require a sufficient mass transfer of substrate to their locations for unrestricted degradation activity. The results show that aggregation of the bacterial cells indeed led to a major reduction in the degradation activity of the entire bacterial population due to more severe restrictions of substrate bioavailability. Bacterial densities considered in the simulations were in agreement with measured densities for groundwater systems [59], [61], [62], [80]–[83], especially when considering the variability of biomass concentrations between individual pores. It has also been shown that the spatial distribution of microorganisms in an aquifer exhibits strong heterogeneities down to the micro-scale [9], [15]. Furthermore, acetate and toluene chosen as more or less readily degradable substrates in this study are organic compounds commonly found in (contaminated) groundwater either as metabolites of other degradation processes [67], [83]–[85] or as anthropogenic contaminants [67]. Thus, the effects presented in our study should be representative of real world aquifers. Measured concentrations of bacterial cells/biomass representing average values of a macro-scale sample may thus miserably fail to predict the *in situ* bacterial degradation potential: in addition to limitations caused by mass transfer from the aqueous phase to the pore walls [6], [16], [17], or by variation of biomass concentration between pores [74], [78], we show that the aggregation of cells inside single pores is a major factor to be considered [86]–[89]. More experimental data on the *in situ* distribution of bacteria at the micro-scale

would be beneficial for determining the degree of aggregation to be expected in a given natural porous medium. However, given that most bacteria grow into clusters of cells upon attachment to surfaces, unless they have specific surface motility mechanisms, it is likely that the colony scenarios with their reduced bioavailability are the rule rather than the exception.

Results show that the substrate concentration did not decrease immediately to zero at the colony surface (Figure 3 and SI 4). Thus, the colony thickness did impact biodegradation. The algorithm used in this study to generate the colonies and their specific sizes resulted in approximately symmetric colonies of constant cell density. One could consider additional factors such as shear forces or feedbacks between colony properties (e.g., EPS content or positioning of new cells) and colony growth that may result in more complex colony shapes and thicknesses, but such aspects were beyond the scope of the present study.

Results of this study show that when bacteria form colony-like aggregates both the mass transfer to the colony as well as the reactive transport processes within the colony have an impact on pore-scale degradation rates. In addition to the discontinuous distribution of the biomass, this questions the use of simplifications (e.g., (rough) reactive surfaces or dual-porosity approaches) that consider only one of these rate-limiting processes.

To obtain a more general quantitative assessment of the influence of biomass aggregation/colony formation on *in situ* biodegradation in aquifers or other water-saturated porous media, the high-resolution 2D simulations were used to constrain the effective rate expression describing biodegradation along a 1D flow path. Results

show that this effective-rate concept introduced for biofilm-like biomass distributions [16], [17], can also be adapted to consider the formation of aggregates. For the more realistic representation of colonies and their distribution by discontinuous reactive zones, the obtained effective colony sizes show a very coherent result since only the number of cells/colony determined the effective colony size. For establishing a generally applicable functional relationship predicting the effective colony size for a given system, more simulations would be needed but the results shown indicate the existence of such a relationship and present a way to determine it. For the more abstract representation of colonies as a continuous reactive section of modified reactivity – which could more easily be implemented in reactive transport approaches for the macro-scale – the obtained effective colony sizes (and thus reactivities) allow only for a weaker link between cells/colony and apparent colony size. Nevertheless, this approach still allows a rough estimate of the resulting degradation rates and provides a route to consider the effect of colony formation in upscaled rate expressions for the macro-scale.

Furthermore, the combination of high-resolution 2D simulations with 1D simulations using effective rate expressions enabled a quantification of effective bioavailabilities. These results confirm the strong impact of the micro-scale biomass distribution on substrate bioavailability. They show that even in cases where mass transfer toward a continuous biofilm along the pore wall would not impose major restrictions on bioavailability (i.e., high B_{eff}(colony) values), the additional effect of biomass aggregation can lead to a more severe limitation of bioavailability (i.e., much lower B_{eff}(colony) values; Figure 6). In the scenarios considered here, effective bioavailability reductions of up to more than one order of magnitude were observed,

showing that *in situ* degradation rates were highly affected by the micro-scale distribution of biomass.

The Péclet number (*Pe*) represents the ratio between the time scales of convection and diffusion [90]. For *Pe* > 6, advection dominates, while diffusion is the important driver for *Pe* < 6 [91]. The range of velocities investigated here resulted in *Pe* ranging from 1.5 to 24, thus covering a representative set of conditions ranging from diffusion-dominated to advection-dominated. The investigated conditions were well within the range of Péclet numbers typical for groundwater, covering fine sand to gravel [92]. The dimensionless Damköhler (*Da*) number relates the time scales of reaction and of advective transport. A system is reaction rate-limited if *Da* << 1 and it is mass transport-limited if *Da* >> 1, which is the case for the scenarios presented here, where numbers ranged from 13 to 210. These numbers were also representative for fast reactions [93] in a coarse/ medium sand aquifer [23]. The dimensionless Thiele modulus Φ^2 relates the time scales of reaction and diffusive transport [94] and is therefore more appropriate for biomass than the Damköhler number. In the colonies, Φ^2 ranged between 0.6 and 80, which broadly falls within the transition between reaction (low Φ^2) and diffusion limited regimes (high Φ^2) [16]. These values are similar to Φ^2-values of 0.4-18 reported reactive antimicrobial agents in a biofilm [95].

The present study analysed processes within a cross section of a pore of regular geometry, which is certainly a severe simplification of the pore structure in a natural porous medium and of the flow and transport therein. Also, for *Pe* < 10 as considered for some of the scenarios, preferential flow can be assumed to occur [96]. Similarly,

microbial activity is restricted here to the degradation of a single substrate, no other factors than the substrate concentration are assumed to affect this degradation activity, colonies consist only of bacterial cells and no extracellular polymeric substances (EPS), and would – if extrapolated – be effectively rings around the 3D pore, instead of discrete three dimensional colonies. However, such simplifications have been shown to provide valuable information on the dynamics of bacterial systems [14], [16], [97]–[100]. They have been extended and applied to pore networks as well [43], [101]–[107]. These simplifications allow determining the relevance of the studied processes without confounding effects. Furthermore, these simplifications enabled the systematic comparison of the 2D simulations with effective rate-law expressions that provide the means for an upscaling of the obtained results to pore networks and beyond. Such scalable results provide the opportunity to study the influence of bacterial distribution heterogeneity at larger scales especially when microbial abundance is positively [108] or negatively [109] correlated with flow velocity. In particular, the obtained effective rate expressions allow for the consideration of micro-scale biomass aggregations in modelling approaches simulating processes in networks of interconnected pores [110]. Nevertheless, further research is needed to test and verify the developed effective rate expression in the presence of more complex conditions than considered in this study and whether the presented concept and the 2D fluid dynamics computations can be applied analogously in larger systems such as pore networks.

In summary, the results of the present study demonstrate the impact that microbial distribution patterns even at the micro-scale have on substrate bioavailability and *in situ* biodegradation rates and provide a conceptual approach how these results may be

scaled up. This proof-of-principle study can be adapted to more complex scenarios in the future to study how the properties at the system level emerge from the distribution of the individual cells and their adaptive behaviour [111].

Acknowledgements

Funding: This work was supported by the European Community's Seventh Framework Programme (FP7/2007-2013) [grant number 235834 to SIS and JUK]; and the Ministerium für Wissenschaft, Weiterbildung und Kultur Rheinland-Pfalz, Germany ["Research initiative", project AufLand].

Supporting Information available

Additional information on the model setup, the conversion of cell concentrations, the origin of parameter values, and additional results for alternative averaging approaches and non-base case scenarios.

References

[1] R. U. Meckenstock, M. Elsner, C. Griebler, T. Lueders, C. Stumpp, J. Aamand, S. N. Agathos, H.-J. Albrechtsen, L. Bastiaens, P. L. Bjerg, N. Boon, W. Dejonghe, W. E. Huang, S. I. Schmidt, E. Smolders, S. R. Sørensen, D. Springael, and B. M. van Breukelen, "Biodegradation: Updating the concepts of control for microbial cleanup in contaminated aquifers," *Environ. Sci. Technol.*, vol. 49, no. 12, pp. 7073–7081, 2015.

[2] S. I. Schmidt, M. Schwientek, and M. O. Cuthbert, "Towards an integrated understanding of how micro scale processes shape groundwater ecosystem

functions," *Sci. Total Environ.*, vol. 592, pp. 215–227, 2017.

[3] N. W. Haws, W. P. Ball, and E. J. Bouwer, "Modeling and interpreting bioavailability of organic contaminant mixtures in subsurface environments," *J. Contam. Hydrol.*, vol. 82, no. 3–4, pp. 255–292, 2006.

[4] O. Cirpka and A. Valocchi, "Two-dimensional concentration distribution for mixing-controlled bioreactive transport in steady state," *Adv. Water Resour.*, vol. 30, no. 6–7, pp. 1668–1679, Jun. 2007.

[5] D. S. Raje and V. Kapoor, "Experimental study of bimolecular reaction kinetics in porous media," *Environ. Sci. Technol.*, vol. 34, no. 7, pp. 1234–1239, 2000.

[6] T. N. P. Bosma, P. J. M. Middeldorp, G. Schraa, and A. J. B. Zehnder, "Mass transfer limitation of biotransformation: Quantifying bioavailability," *Env. Sci Technol*, vol. 31, no. 1, pp. 248–252, 1997.

[7] H. Harms and T. N. P. Bosma, "Mass transfer limitation of microbial growth and pollutant degradation," *J. Ind. Microbiol. Biotechnol.*, vol. 18, no. 2–3, pp. 97–105, 1997.

[8] C. E. Knutson, C. J. Werth, and A. J. Valocchi, "Pore-scale simulation of biomass growth along the transverse mixing zone of a model two-dimensional porous medium," *Water Resour. Res.*, vol. 41, p. W07007, 2005.

[9] R. W. Harvey, R. L. Smith, and L. George, "Effect of organic contamination upon microbial distributions and heterotrophic uptake in a Cape Cod, Mass., aquifer," *Appl. Environ. Microbiol.*, vol. 48, no. 6, pp. 1197–1202, 1984.

[10] B. A. Bekins, E. M. Godsy, and E. Warren, "Distribution of microbial physiologic types in an aquifer contaminated by crude oil," *Microb. Ecol.*, vol. 37, pp. 263–275, 1999.

[11] R. M. Lehman, F. S. Colwell, and G. A. Bala, "Attached and unattached microbial communities in a simulated basalt aquifer under fracture- and porous-flow conditions," *Appl. Environ. Microbiol.*, vol. 67, no. 6, pp. 2799–2809, 2001.

[12] C. Griebler, B. Mindl, D. Slezak, and M. Geiger-Kaiser, "Distribution patterns of attached and suspended bacteria in pristine and contaminated shallow aquifers studied with an in situ sediment exposure microcosm," *Aquat. Microb. Ecol.*, vol. 28, no. 2, pp. 117–129, 2002.

[13] A. Iribar, J. M. Sánchez-Pérez, E. Lyautey, and F. Garabétian, "Differentiated free-living and sediment-attached bacterial community structure inside and outside denitrification hotspots in the river–groundwater interface," *Hydrobiologia*, vol. 598, no. 1, pp. 109–121, Sep. 2008.

[14] H. J. Dupin, P. K. Kitanidis, and P. L. McCarty, "Pore-scale modeling of biological clogging due to aggregate expansion: a material mechanics approach," *Water Resour. Res.*, vol. 37, no. 12, pp. 2965–2979, 2001.

[15] G. C. Iltis, R. T. Armstrong, D. P. Jansik, B. D. Wood, and D. Wildenschild, "Imaging biofilm architecture within porous media using synchrotron-based X-ray computed microtomography," *Water Resour. Res.*, vol. 47, no. W02601, pp. 1–5, Feb. 2011.

[16] F. Heße, F. A. Radu, M. Thullner, and S. Attinger, "Upscaling of the advection–diffusion–reaction equation with Monod reaction," *Adv. Water Resour.*, vol. 32, no. 8, pp. 1336–1351, 2009.

[17] F. Hesse, H. Harms, S. Attinger, and M. Thullner, "Linear exchange model for the description of mass transfer limited bioavailability at the pore scale," *Environ. Sci. Technol.*, vol. 44, no. 6, pp. 2064–2071, 2010.

[18] I. Battiato, D. M. Tartakovsky, A. M. Tartakovsky, and T. Scheibe, "On breakdown of macroscopic models of mixing-controlled heterogeneous reactions in porous media," *Adv. Water Resour.*, vol. 32, no. 11, pp. 1664–1673, 2009.

[19] F. J. Molz, M. A. Widdowson, and L. D. Benefield, "Simulation of microbial growth dynamics coupled to nutrient and oxygen-transport in porous media," *Water Resour. Res.*, vol. 22, no. 8, pp. 1207–1216, 1986.

[20] P. Baveye and A. Valocchi, "An evaluation of mathematical models of the transport of biologically reacting solutes in saturated soils and aquifers," *Water Resour. Res.*, vol. 25, no. 6, pp. 1413–1421, 1989.

[21] M. Thullner, P. Regnier, and P. Van Cappellen, "Modeling microbially induced carbon degradation in redox-stratified subsurface environments: concepts and open questions," *Geomicrobiol. J.*, vol. 24, no. 3, pp. 139–155, Apr. 2007.

[22] B. D. Wood, K. Radakovich, and F. Golfier, "Effective reaction at a fluid–solid interface: Applications to biotransformation in porous media," *Adv. Water Resour.*, vol. 30, pp. 1630–1647, Jun. 2007.

[23] F. Golfier, B. D. Wood, L. Orgogozo, M. Quintard, and M. Buès, "Biofilms in porous media: Development of macroscopic transport equations via volume averaging with closure for local mass equilibrium conditions," *Adv. Water Resour.*, vol. 32, no. 3, pp. 463–485, 2009.

[24] L. Orgogozo, F. Golfier, M. A. Buès, M. Quintard, and T. Koné, "A dual-porosity theory for solute transport in biofilm-coated porous media," *Adv. Water Resour.*, vol. 62, pp. 266–279, 2013.

[25] J. B. Best, "The interference of intracellular enzymatic properties from kinetic data obtained on living cells. 1. Some kinetic considerations regarding an

enzyme enclosed by a diffusion barrier," *J. Cell. Comp. Physiol.*, vol. 46, pp. 1–27, 1955.

[26] P. E. Kechagia, I. N. Tsimpanogiannis, Y. C. Yortsos, and P. C. Lichtner, "On the upscaling of reaction-transport processes in porous media with fast or finite kinetics," *Chem. Eng. Sci.*, vol. 57, no. 13, pp. 2565–2577, 2002.

[27] V. Balakotaiah and H. C. Chang, "Dispersion of chemical solutes in chromatographs and reactors," *Philos. Trans. R. Soc. London Ser. A-Mathematical Phys. Eng. Sci.*, vol. 351, no. 1695, pp. 39–75, 1995.

[28] L. Li, C. A. Peters, and M. A. Celia, "Upscaling geochemical reaction rates using pore-scale network modeling," vol. 29, pp. 1351–1370, 2006.

[29] V. Jikov, S. Kozlov, and O. Oleinik, *Homogenization of differential operators and integral functionals*. Berlin: Springer, 1995.

[30] E. Weinan, B. Engquist, X. Li, and W. Ren, "The heterogeneous multiscale method: A review," *Commun. Comput. Phys.*, vol. 2, no. 3, pp. 367–450, 2007.

[31] S. Veran, Y. Aspa, and M. Quintard, "Effective boundary conditions for rough reactive walls in laminar boundary layers," *Int. J. Heat Mass Transf.*, vol. 52, no. 15–16, pp. 3712–3725, 2009.

[32] G. Deolmi, W. Dahmen, and S. M. Uller, "Effective boundary conditions for compressible flows over rough boundaries," *Commun. Comput. Phys.*, vol. 21, no. 2, pp. 358–400, 2017.

[33] L. A. Lardon, B. V. Merkey, S. Martins, A. Dötsch, C. Picioreanu, J. U. Kreft, and B. F. Smets, "iDynoMiCS: Next-generation individual-based modelling of biofilms," *Environ. Microbiol.*, vol. 13, no. 9, pp. 2416–2434, 2011.

[34] T. Cordt and H. Kussmaul, "Characterization of some organic acids in the subsurface of the Sandhausen ecosystem," in *Progress in Hydrogeochemistry*,

G. Matthess, F. Frimmel, P. Hirsch, H. D. Schulz, and H. E. Usdowski, Eds. Berlin: Springer Verlag, 1992, pp. 93–100.

[35] CRC, *Handbook of Chemistry and Physics*, 91st editi. CRC Press, 2011.

[36] L. Korson, W. Drost-Hansen, and F. J. Millero, "Viscosity of water at various temperatures," *J. Phys. Chem.*, vol. 73, no. 1, pp. 34–39, 1969.

[37] J. Gerritse, F. Schut, and J. C. Gottschal, "Modelling of mixed chemostat cultures of an aerobic bacterium, Comamonas testosteroni, and an anaerobic bacterium, Veillonella alcalescens: comparison with experimental data.," *Appl. Environ. Microbiol.*, vol. 58, no. 5, pp. 1466–76, May 1992.

[38] A. R. Pedersen, S. Møller, S. Molin, and E. Arvin, "Activity of toluene-degrading Pseudomonas putida in the early growth phase of a biofilm for waste gas treatment.," *Biotechnol. Bioeng.*, vol. 54, no. 2, pp. 131–41, Apr. 1997.

[39] C. Picioreanu, M. C. M. van Loosdrecht, T. P. Curtis, and K. Scott, "Model based evaluation of the effect of pH and electrode geometry on microbial fuel cell performance," *Bioelectrochemistry*, vol. 78, no. 1, pp. 8–24, 2010.

[40] J.-U. Kreft, C. Picioreanu, J. W. T. Wimpenny, and M. C. M. Van Loosdrecht, "Individual-based modelling of biofilms," *Microbiology*, vol. 147, pp. 2897–2912, 2001.

[41] C. Picioreanu, J.-U. Kreft, and M. C. M. van Loosdrecht, "Particle-based multidimensional multispecies biofilm model," *Appl. Environ. Microbiol.*, vol. 70, no. 5, pp. 3024–3040, 2004.

[42] J. B. Xavier, C. Picioreanu, and M. C. M. van Loosdrecht, "Framework for multidimensional biofilm modelling," *Environ. Microbiol.*, vol. 7, no. 8, pp. 1085–1103, 2005.

[43] M. Thullner and P. Baveye, "Computational pore network modeling of the

influence of biofilm permeability on bioclogging in porous media," *Biotechnol. Bioeng.*, vol. 99, no. 6, pp. 1337–1351, 2008.

[44] J. Dockery and I. Klapper, "Finger formation in biofilm layers," *SIAM J. Appl. Math.*, vol. 62, no. 3, pp. 853–869, 2001.

[45] N. G. Cogan, "Two-fluid model of biofilm disinfection," *Bull. Math. Biol.*, vol. 70, no. 3, pp. 800–819, 2008.

[46] P. Cumsille, J. A. Asenjo, and C. Conca, "A novel model for biofilm growth and its resolution by using the hybrid immersed interface-level set method," *Comput. Math. with Appl.*, vol. 67, no. 1, pp. 34–51, 2014.

[47] W. Kinzelbach, W. Schäfer, and J. Herzer, "Numerical modeling of natural and enhanced denitrification processes in aquifers.," *Water Resour. Res.*, vol. 27, p. 1123–1135., 1991.

[48] D. A. Graf von der Schulenburg, T. R. R. Pintelon, C. Picioreanu, M. C. M. van Loosdrecht, and M. L. Johns, "Three-dimensional simulations of biofilm growth in porous media," *AIChE J.*, vol. 55, no. 2, 2009.

[49] C. Picioreanu, J. S. S. Vrouwenvelder, and M. C. M. van Loosdrecht, "Three-dimensional modeling of biofouling and fluid dynamics in feed spacer channels of membrane devices," *J. Memb. Sci.*, vol. 345, no. 1–2, pp. 340–354, Dec. 2009.

[50] A. I. Radu, J. S. Vrouwenvelder, M. C. M. van Loosdrecht, and C. Picioreanu, "Modeling the effect of biofilm formation on reverse osmosis performance: Flux, feed channel pressure drop and solute passage," *J. Memb. Sci.*, vol. 365, no. 1–2, pp. 1–15, Dec. 2010.

[51] K. J. Martin, C. Picioreanu, and R. Nerenberg, "Multidimensional modeling of biofilm development and fluid dynamics in a hydrogen-based, membrane

biofilm reactor (MBfR)," *Water Res.*, vol. 47, no. 13, pp. 4739–4751, 2013.

[52] R Development Core Team, "R: A language and environment for statistical computing." R Foundation for Statistical Computing, Vienna, Austria, 2016.

[53] D. Sarkar, *Lattice: Multivariate Data Visualization with R*. New York: Springer, 2008.

[54] H. Wickham, *ggplot2: Elegant graphics for data analysis*. New York: Springer, 2009.

[55] D. R. Aguilera, P. Jourabchi, C. Spiteri, and P. Regnier, "A knowledge-based reactive transport approach for the simulation of biogeochemical dynamics in Earth systems," *Geochemistry, Geophys. Geosystems*, vol. 6, no. 7, pp. 1–18, 2005.

[56] M. Thullner, P. van Cappellen, and P. Regnier, "Modeling the impact of microbial activity on redox dynamics in porous media," *Geochim. Cosmochim. Acta*, vol. 69, no. 21, pp. 5005–5019, Nov. 2005.

[57] M. Kampara, M. Thullner, H. H. Richnow, H. Harms, and L. Y. Wick, "Impact of bioavailability restrictions on microbially induced stable isotope fractionation. 2. Experimental evidence," *Environ. Sci. Technol.*, vol. 42, no. 17, pp. 6544–6551, 2008.

[58] T. Fenchel, *Ecology of Protozoa*. Berlin; Madison: Springer-Verlag; Science Tech Publishers, 1987.

[59] J. T. Wilson, J. F. McNabb, D. L. Balkwill, and W. C. Ghiorse, "Enumeration and morphological characterization of bacteria indigenous to subsurface environments," *Ground Water*, vol. 21, no. 2, pp. 134–142, 1983.

[60] J. Marxsen, "Investigations into the number of respiring bacteria in groundwater from sandy and gravelly deposits," *Microb. Ecol.*, vol. 16, pp. 65–

72, 1988.

[61] B. Zarda, G. Mattison, A. Hess, D. Hahn, P. Höhener, and J. Zeyer, “Analysis of bacterial and protozoan communities in an aquifer contaminated with monoaromatic hydrocarbons,” *FEMS Microbiol. Ecol.*, vol. 27, pp. 141–152, 1998.

[62] M. A. Barlaz, D. M. Schaefer, and R. K. Ham, “Bacterial population development and chemical characteristics of refuse decomposition in a simulated sanitary landfill,” *Appl. Environ. Microbiol.*, vol. 55, pp. 55–65, 1989.

[63] L. G. Ljungdahl, “The autotrophic pathway of acetate synthesis in acetogenic bacteria.,” *Annu. Rev. Microbiol.*, vol. 40, pp. 415–50, 1986.

[64] R. G. Mattison, H. Taki, and S. Harayama, “The soil flagellate Heteromita globosa accelerates bacterial degradation of alkylbenzenes through grazing and acetate excretion in batch culture,” *Microb. Ecol.*, vol. 49, no. 1, pp. 142–50, Jan. 2005.

[65] G. Michal and D. Schomburg, *Biochemical pathways: an atlas of biochemistry and molecular biology*, 2nd editio. Hoboken, New Jersey: John Wiley & Sons, Inc., 2012.

[66] F. Gründger, N. Jiménez, T. Thielemann, N. Straaten, T. Lüders, H. H. Richnow, F. Gründger, N. Jiménez, T. Thielemann, N. Straaten, H. Richnow, and M. Krüger, “Microbial methane formation in deep aquifers of a coal-bearing sedimentary basin, Germany,” *Front. Microbiol.*, vol. 6, 2015.

[67] K. N. Timmis, *Handbook of Hydrocarbon and Lipid Microbiology*. Berlin: Springer, 2010.

[68] C. Winderl, B. Anneser, C. Griebler, R. U. Meckenstock, and T. Lueders,

"Depth-resolved quantification of anaerobic toluene degraders and aquifer microbial community patterns in distinct redox zones of a tar oil contaminant plume.," *Appl. Environ. Microbiol.*, vol. 74, no. 3, pp. 792–801, Mar. 2008.

[69] B. Anneser, F. Einsiedl, R. U. Meckenstock, L. Richters, F. Wisotzky, and C. Griebler, "High-resolution monitoring of biogeochemical gradients in a tar oil-contaminated aquifer," *Appl. Geochemistry*, vol. 23, no. 6, pp. 1715–1730, Jun. 2008.

[70] R. D. Bauer, M. Rolle, P. Kürzinger, P. Grathwohl, R. U. Meckenstock, and C. Griebler, "Two-dimensional flow-through microcosms – Versatile test systems to study biodegradation processes in porous aquifers," *J. Hydrol.*, vol. 369, no. 3–4, pp. 284–295, May 2009.

[71] R. D. Bauer, P. Maloszewski, Y. Zhang, R. U. Meckenstock, and C. Griebler, "Mixing-controlled biodegradation in a toluene plume--results from two-dimensional laboratory experiments.," *J. Contam. Hydrol.*, vol. 96, no. 1–4, pp. 150–68, Feb. 2008.

[72] A. Herzyk, L. Fillinger, M. Larentis, S. Qiu, P. Maloszewski, M. Hünniger, S. I. Schmidt, C. Stumpp, S. Marozava, P. S. K. Knappett, M. Elsner, R. Meckenstock, T. Lueders, and C. Griebler, "Response and recovery of a pristine groundwater ecosystem impacted by toluene contamination – A meso-scale indoor aquifer experiment," *J. Contam. Hydrol.*, vol. 207, pp. 17–30, 2017.

[73] M. Hünniger, S. I. Schmidt, N. Peuckmann, and P. Maloszewski, "Experimental and mathematical methods to quantify the water flux and the transport processes in heterogeneous aquifer model systems," *IAHS Publ.*, vol. 342, no. Proceedings of the 7th International Groundwater Quality Conference,

Zurich, Switzerland, 13-18 June 2010, pp. 180–183, 2011.

[74] M. Gharasoo, F. Centler, P. Regnier, H. Harms, and M. Thullner, "A reactive transport modeling approach to simulate biogeochemical processes in pore structures with pore-scale heterogeneities," *Environ. Model. Softw.*, vol. 30, pp. 102–114, Apr. 2012.

[75] G. D. Tartakovsky, A. M. Tartakovsky, T. D. Scheibe, Y. Fang, R. Mahadevan, and D. R. Lovley, "Pore-scale simulation of microbial growth using a genome-scale metabolic model: Implications for Darcy-scale reactive transport," *Adv. Water Resour.*, vol. 59, pp. 256–270, Sep. 2013.

[76] C. Poll, J. I. Ingwersen, M. S. Stemmer, M. H. G. Gerzabek, and E. K. Kandeler, "Mechanisms of solute transport affect small-scale abundance and function of soil microorganisms in the detritusphere," *Eur. J. Soil Sci.*, vol. 57, pp. 583–595, 2006.

[77] S. Bottero, T. Storck, T. J. Heimovaara, M. C. M. van Loosdrecht, M. V Enzien, and C. Picioreanu, "Biofilm development and the dynamics of preferential flow paths in porous media.," *Biofouling*, vol. 29, no. 9, pp. 1069–86, 2013.

[78] F. Centler, I. Fetzer, and M. Thullner, "Modeling population patterns of chemotactic bacteria in homogeneous porous media.," *J. Theor. Biol.*, vol. 287, pp. 82–91, Oct. 2011.

[79] A. Dechesne, M. Owsianiak, A. Bazire, G. L. Grundmann, P. J. Binning, and B. F. Smets, "Biodegradation in a partially saturated sand matrix: Compounding effects of water content, bacterial spatial distribution, and motility," *Environ. Sci. Technol.*, vol. 44, no. 7, pp. 2386–2392, 2010.

[80] J. Marxsen, "Ein neues Verfahren zur Untersuchung der bakteriellen

Besiedlung grundwasserführender sandiger Sedimente," *Arch. Hydrobiol.*, vol. 95, no. 1/4, pp. 221–233, 1982.

[81] D. M. Akob and K. Küsel, "Where microorganisms meet rocks in the Earth's Critical Zone," *Biogeosciences*, vol. 8, no. 12, pp. 3531–3543, Dec. 2011.

[82] A. Rizoulis, D. R. Elliott, S. A. Rolfe, S. F. Thornton, S. A. Banwart, R. W. Pickup, and J. D. Scholes, "Diversity of planktonic and attached bacterial communities in a phenol-contaminated sandstone aquifer.," *Microb. Ecol.*, vol. 66, no. 1, pp. 84–95, Jul. 2013.

[83] A. Grabowski, O. Nercessian, F. Fayolle, D. Blanchet, and C. Jeanthon, "Microbial diversity in production waters of a low-temperature biodegraded oil reservoir," *FEMS Microbiol. Ecol.*, vol. 54, no. 3, pp. 427–443, Nov. 2005.

[84] S. F. Thornton, S. Quigley, M. J. Spence, S. A. Banwart, S. Bottrell, and D. N. Lerner, "Processes controlling the distribution and natural attenuation of dissolved phenolic compounds in a deep sandstone aquifer," *J. Contam. Hydrol.*, vol. 53, pp. 233–267, 2001.

[85] E. M. Thurman, *Organic geochemistry of natural waters*. Dordrecht, The Netherlands: Martinus Nijhoff, 1985.

[86] J. E. Keymer, P. Galajda, C. Muldoon, S. Park, and R. H. Austin, "Bacterial metapopulations in nanofabricated landscapes," *PNAS*, vol. 103, no. 46, pp. 17290–17295, 2006.

[87] M. Gharasoo, F. Centler, I. Fetzer, and M. Thullner, "How the chemotactic characteristics of bacteria can determine their population patterns," *Soil Biol. Biochem.*, vol. 69, pp. 346–358, Feb. 2014.

[88] Y. Kuzyakov and E. Blagodatskaya, "Microbial hotspots and hot moments in soil: Concept & review," *Soil Biol. Biochem.*, vol. 83, pp. 184–199, 2015.

[89] L. S. Ruamps, N. Nunan, and C. Chenu, "Microbial biogeography at the soil pore scale," *Soil Biol. Biochem.*, vol. 43, no. 2, pp. 280–286, 2011.

[90] C. R. Fitts, *Groundwater Science*, Second Edi. Amsterdam: Elsevier, 2012.

[91] D. K. Burnell, J. W. Mercer, and L. S. Sims, "Analytical models of steady-state plumes undergoing sequential first-order degradation," *Ground Water*, vol. 50, no. 3, pp. 394–411, 2012.

[92] A. D. Chiasson, S. J. Rees, and J. D. Spitler, "A preliminary assessment of the effects of groundwater flow on closed-loop ground-source heat pump systems," *ASHRAE Trans.*, vol. 106, no. 1, pp. 380–393, 2000.

[93] M. Dentz, T. Le Borgne, A. Englert, and B. Bijeljic, "Mixing, spreading and reaction in heterogeneous media: A brief review," *J. Contam. Hydrol.*, vol. 120–121, pp. 1–17, 2011.

[94] R. B. Bird, W. E. Stewart, and E. N. Lightfoot, *Transport Phenomena*, 2nd ed. John Wiley & Sons, Inc., 2006.

[95] P. S. Stewart and J. B. Raquepas, "Implications of reaction-diffusion theory for the disinfection of microbial biofilms by reactive antimicrobial agents," *Chem. Eng. Sci.*, vol. 50, no. 19, pp. 3099–3104, 1995.

[96] M. Kühn, *Reactive flow modeling of hydrothermal systems*. Springer Science & Business Media, 2004.

[97] K. Stolpovsky, P. Martinez-Lavanchy, H. J. Heipieper, P. Van Cappellen, and M. Thullner, "Incorporating dormancy in dynamic microbial community models," *Ecol. Modell.*, vol. 222, no. 17, pp. 3092–3102, Sep. 2011.

[98] S. König, A. Worrich, F. Centler, L. Y. Wick, A. Miltner, M. K. Astner, M. Thullner, K. Frank, and T. Banitz, "Modelling functional resilience of microbial ecosystems: analysis of governing processes," *Environ. Model.*

Softw., vol. 89, pp. 31–39, 2017.

[99] C. Kaiser, O. Franklin, U. Dieckmann, and A. Richter, "Microbial community dynamics alleviate stoichiometric constraints during litter decay," *Ecol. Lett.*, vol. 17, no. 6, pp. 680–690, 2014.

[100] R. D. Bauer, M. Rolle, S. Bauer, C. Eberhardt, P. Grathwohl, O. Kolditz, R. U. Meckenstock, and C. Griebler, "Enhanced biodegradation by hydraulic heterogeneities in petroleum hydrocarbon plumes," *J. Contam. Hydrol.*, vol. 105, no. 1–2, pp. 56–68, Feb. 2009.

[101] K. Stolpovsky, M. Gharasoo, and M. Thullner, "The impact of pore-size heterogeneities on the spatiotemporal variation of microbial metabolic activity in porous media," *Soil Sci.*, vol. 177, no. 2, pp. 98–110, 2012.

[102] E. L. King, K. Tuncay, P. Ortoleva, and C. Meile, "Modeling biogeochemical dynamics in porous media: Practical considerations of pore scale variability, reaction networks, and microbial population dynamics in a sandy aquifer," *J. Contam. Hydrol.*, vol. 112, no. 1–4, pp. 130–140, 2010.

[103] T. Banitz, I. Fetzer, K. Johst, L. Y. Wick, H. Harms, and K. Frank, "Assessing biodegradation benefits from dispersal networks," *Ecol. Modell.*, vol. 222, no. 14, pp. 2552–2560, 2011.

[104] A. Ebrahimi and D. Or, "Hydration and diffusion processes shape microbial community organization and function in model soil aggregates," *Water Resour. Res.*, vol. 51, pp. 9804–9827, 2015.

[105] M. Thullner, J. Zeyer, and W. Kinzelbach, "Influence of microbial growth on hydraulic properties of pore networks," *Transp. Porous Media*, vol. 49, pp. 99–122, 2002.

[106] I. Battiato, D. M. Tartakovsky, A. M. Tartakovsky, and T. D. Scheibe, "Hybrid

models of reactive transport in porous and fractured media," *Adv. Water Resour.*, vol. 34, no. 9, pp. 1140–1150, Sep. 2011.

[107] Y. Tang, A. J. Valocchi, and C. J. Werth, "A hybrid pore-scale and continuum-scale model for solute diffusion, reaction, and biofilm development in porous media," *Water Resour. Res.*, vol. 6, no. 4, pp. 1846–1859, 2015.

[108] M. Bundt, F. Widmer, M. Pesaro, J. Zeyer, and P. Blaser, "Preferential flow paths: Biological 'hot spots' in soils," *Soil Biol. Biochem.*, vol. 33, no. 6, pp. 729–738, 2001.

[109] I. M. Nambi, C. Werth, R. A. Sanford, and A. J. Valocchi, "Pore-scale analysis of anaerobic halorespiring bacterial growth along the transverse mixing zone of an etched silicon pore network," *Environ. Sci. Technol.*, vol. 37, no. 24, pp. 5617–5624, 2003.

[110] Q. Xiong, T. Baychev, and A. P. Jivkov, "Review of pore network modelling of porous media: experimental characterisations, network constructions and applications to reactive transport," *J. Contam. Hydrol.*, vol. 192, pp. 101–117, 2016.

[111] V. Grimm, U. Berger, F. Bastiansen, S. Eliassen, V. Ginot, J. Giske, J. Goss-Custard, T. Grand, S. K. Heinz, and G. Huse, "A standard protocol for describing individual-based and agent-based models," *Ecol. Modell.*, vol. 198, no. 1–2, pp. 115–126, Sep. 2006.